ChemComm

COMMUNICATION

View Article Online
View Journal | View Issue

Open Access Article. Published on 03 December 2024. Downloaded on 8/9/2025 5:24:47 PM.
This article is licensed under a Creative Commons Attribution 3.0 Unported Licence.

Check for updates

Cite this: *Chem. Commun.*, 2025, **61**, 149

Received 28th September 2024,
Accepted 28th November 2024

DOI: 10.1039/d4cc05067c

rsc.li/chemcomm

Cationic groups in polystyrene/O-PBI blends influence performance and hydrogen crossover in AEMWE†

Linus Hager, *[ab] Maximilian Schrodt,[ab] Manuel Hegelheimer,[ab] Julian Stonawski,[ab] Pradipkumar Leuaa,[c] Christodoulos Chatzichristodoulou,[c] Andreas Hutzler,[a] Thomas Böhm,[a] Simon Thiele[ab] and Jochen Kerres *[ad]

This study examines the effect of various quaternary ammonium groups on AEMWE performance and hydrogen crossover in blends of quaternized polystyrenes with O-PBI. Due to their higher hydroxide conductivity (69 mS cm^{-1} at 80 °C, 90% RH), trimethylammonium groups enable AEMWE to reach 1.0 A cm^{-2} at 2.0 V. The trimethylammonium groups exhibit low hydrogen crossover, ranging from 1.5% to 0.3%, across current densities of 50 to 1000 mA cm^{-2}. Low hydrogen crossover is essential for AEMWE in terms of safety and efficiency.

Water electrolysis represents a crucial technology for a future sustainable energy system utilizing green hydrogen as an energy carrier.[1] Anion exchange membrane water electrolysis (AEMWE) is less mature compared to proton exchange membrane water electrolysis (PEMWE) and alkaline water electrolysis (AWE), but it combines advantages from both. AEMWE enables the use of non-platinum group metal (non-PGM) electrocatalysts like AWE and thin dense polymer electrolyte membranes (50–200 μm) like PEMWE, offering the potential for lower capital (CAPEX) and operating costs (OPEX), and increased operational flexibility than any one of the PEMWE and AWE systems.[2] Nevertheless, the widespread adoption of AEMWE is hindered by several challenges: (1) catalyst stability in low KOH concentrations or pure water, (2) long-term membrane durability, (3) scalability (4) low ionic conductivity of anion exchange membranes (AEMs) compared to proton exchange membranes (PEMs).[2,3] Moreover, critical membrane properties, such as hydrogen crossover from the cathode to the anode, are seldom reported in the literature despite their significance for the safety and efficiency of electrolyzers. Recently, we reported on the performance and alkaline stability of blend membranes composed of polystyrenes functionalized with an *N*-methylpiperidinium group attached *via* a C6-spacer and a polybenzimidazole (O-PBI) as a second blend component.[4] This study presents an extended investigation of the impact of cationic groups on the electrochemical properties of such membranes. Our unique membrane preparation approach features a complete absence of fluorine in the polymers and the synthesis process. This is especially relevant in light of increasing environmental concerns and regulatory debates surrounding fluorine-containing chemicals, particularly PFAS, which are known to have detrimental effects on ecosystems and human health.[5] Importantly, some commercial AEMs still comprise alkyl-bound fluorine in the backbone and require large amounts of PFAS in the whole value chain (*e.g.*, PiperION®, Orion®).[6,7]

This study presents the outcome of two key investigations: (1) the synthesis and purification processes for the functionalized monomer 4-(6-bromohexyl)styrene were optimized, enabling its successful homopolymerization. (2) Four different cationic polymers were synthesized, and membranes were prepared from these polymers. Initially, we optimized the synthesis of 4-(6-bromohexyl)styrene (Fig. 1), addressing challenges identified in our previous work and reported in the literature.[4] We increased the excess of 1,6-dibromohexane from initially[4] 4.10 to 10 equivalents to reduce the likelihood of reactions between two Grignard species. This adjustment aimed to decrease the probability of undesired crosslinker formation. We used the difference in vapor pressure between the compounds to purify 4-(6-bromohexyl)-styrene *via* vacuum distillation. 4-(6-Bromohexyl)styrene was obtained with increased purity (Fig. S1, ESI†) compared to the unoptimized reaction and purification conditions. Using ^{1}H-NMR spectroscopy, we confirmed that the crosslinker content was successfully reduced from 3 mol% to less than 1 mol%,

[a] *Forschungszentrum Jülich GmbH, Helmholtz Institute Erlangen-Nürnberg for Renewable Energy (IET-2), Cauerstr. 1, 91058 Erlangen, Germany. E-mail: l.hager@fz-juelich.de, j.kerres@fz-juelich.de*
[b] *Department of Chemical and Biological Engineering, Friedrich Alexander Universität Erlangen-Nürnberg, Egerlandstr. 3, 91058 Erlangen, Germany*
[c] *Department of Energy Conversion and Storage, Technical University of Denmark, Fysikvej, Building 310, 2800 Kongens, Lyngby, Denmark*
[d] *Chemical Resource Beneficiation Faculty of Natural Sciences, North-West University, Potchefstroom 2520, South Africa*

† Electronic supplementary information (ESI) available. See DOI: https://doi.org/10.1039/d4cc05067c

Open Access Article. Published on 03 December 2024. Downloaded on 8/9/2025 5:24:47 PM.
This article is licensed under a Creative Commons Attribution 3.0 Unported Licence.

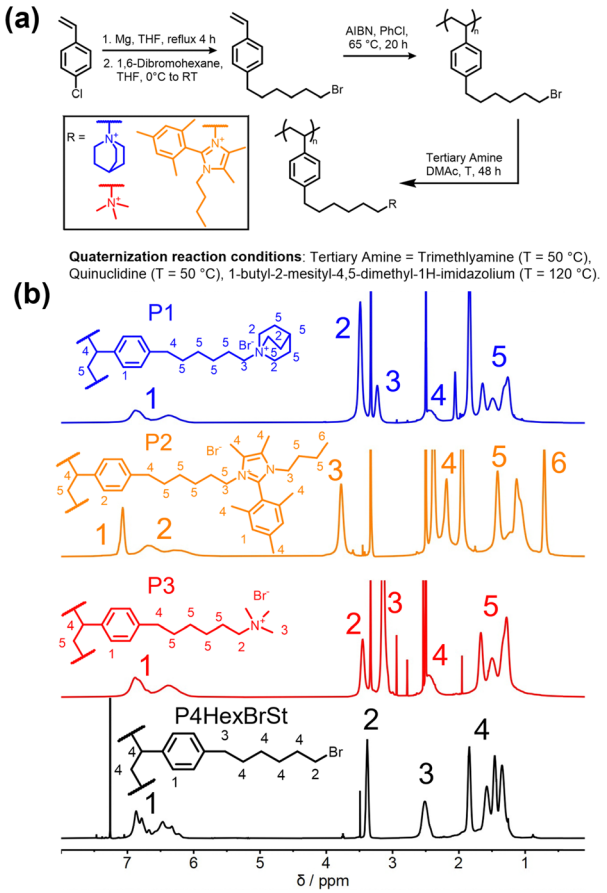

Fig. 1 (a) Schematic representation of the step-by-step reaction pathway: (1) synthesis of the functionalized styrene monomer (2) synthesis of the precursor polymer (3) quaternization with tertiary amines. (b) The ^{1}H-NMR spectra display the quaternized polymers alongside the precursor polymer, highlighting successful quaternization with the respective polymer abbreviations.

enabling the gel-free homopolymerization of 4-(6-bromohexyl)-styrene (Fig. 1a)—a process that was impossible with the monomer mixture containing a higher crosslinker content.[4]

The gel permeation chromatography (GPC) curve (Fig. S4, ESI†) exhibits a molecular weight of 53.7 kg mol^{-1} and a monomodal distribution with a dispersity of 2.06, typical for free radical polymerization. This indicates the absence of crosslinking and smooth polymerizability of the synthesized monomer.

Using tertiary amines, the bromohexyl-functionalized precursor polymer could easily be quaternized in a post-polymerization reaction. In addition to *N*-methylpiperidine, used in our previous study (Pip, P4),[4] other cations were applied, namely quinuclidine (Quin, P1),[8,9] 1-butyl-2-mesityl-4,5-dimethyl-1*H*-imidazole (Im, P2)[10–12] and trimethylamine (TMA, P3),[13] to study the influence of these cations on the membrane properties and the AEMWE performance (polymer abbreviations shown in Fig. 1b). Quantitative quaternization was achieved in all cases, as proven by the ^{1}H NMR spectra (Fig. 1b and Fig. S3, ESI†). These cations were chosen for their high chemical stability in alkaline conditions, essential for AEMWE membranes operating with 1 M KOH.[4,8–12] The selected cations exhibit differences in ionic radii and molecular weight,[10] which are expected to affect the chain packing density of the polymers. This variation in packing density could influence water uptake and hydrogen crossover, which are investigated in this study. The cation size follows the order TMA < Pip ≈ Quin < Im.[10] Although Quin and Pip are approximately the same size, Quin's cage structure may impact packing density, water uptake, and ultimately H_2 crossover.

As a critical property of the novel polymers, the thermal stability of the quaternized polymers and the precursor polymer was measured (Fig. S5, ESI†). Specifically, the precursor polymer (P4HexBrSt) exhibits an onset temperature for thermal degradation at 370 °C, while the quaternized polymers P1, P2, and P3 degrade at 337 °C, 271 °C, and 264 °C, respectively. Thus, all polymers demonstrate sufficient thermal stability for application in an anion exchange membrane water electrolyzer (AEMWE) operating at 70 °C.

Next, blend membranes were prepared by blending the novel cationic polystyrenes with O-PBI (Fig. 2a). A consistent content of 77 wt% of the polystyrene and 23 wt% O-PBI was used for the membranes incorporating Quin, TMA, and Pip designated M1, M3, and M4, respectively. In the case of P2, a higher quaternized polymer content was required due to the significantly lower ion exchange capacity (IEC) of the P2 homopolymer

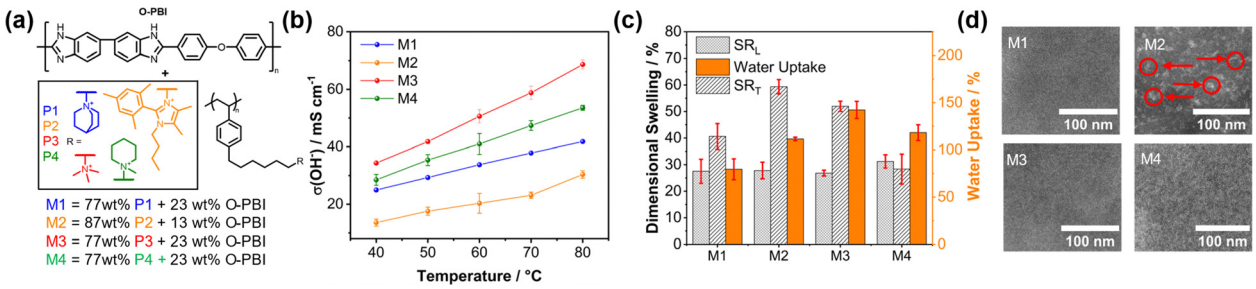

Fig. 2 (a) Structures of the blend components: O-PBI and side-chain functionalized polystyrenes. (b) Temperature-dependent hydroxide conductivity of blend membranes containing 77 wt% of the respective cationic polymer (P1 quinuclidine (Quin), P3 trimethylamine (TMA), and P4 *N*-methylpiperidine (Pip)) in the blend with O-PBI, and 87 wt% of 1-butyl-2-mesityl-4,5-dimethyl-1*H*-imidazole (P2, Im) (c) dimensional swelling and water uptake (WU) of the respective blend membranes, SR_L: in-plane dimensional swelling, SR_T: through-plane dimensional swelling (d) high-angle annular dark field scanning transmission electron microscopy (HAADF-STEM) images of the blend membranes at the same magnification.

Open Access Article. Published on 03 December 2024. Downloaded on 8/9/2025 5:24:47 PM.
This article is licensed under a Creative Commons Attribution 3.0 Unported Licence.

(as indicated in Table S2, ESI†). Additionally, the same membrane as in our previous study, comprising a *N*-methylpiperidinium cation (Pip, P4),[4] was included for comparison (Fig. 2a). Blend membranes were prepared using a method published previously, and the composition was analyzed using ^{1}H NMR and Mohr's titration (Table S2, ESI†). The deviation between the methods stayed below 5%, confirming the accuracy of IEC determination in the blend membranes.

The ionic conductivity scales with the charge carrier density and thus with the IEC. Consequently, the conductivity trends align with the increasing IEC values in the sequence Im (M2) < Quin (M1) < Pip (M4) < TMA (M3) (Fig. 2b). Notably, the highest conductivity of 69 mS cm^{-1} was measured at 80 °C using the TMA cation. M2 exhibits the lowest conductivity resulting from drastically lower IEC due to the high molecular weight of the sterically hindered imidazolium cation. Water uptake (WU) correlates with the membranes' conductivity and swelling ratio (SR) (Fig. 2b). Notably, the membrane properties result from the interplay between both blend components. The hydrophilic ammonium groups drive water uptake, while the hydrophobic O-PBI component enhances mechanical integrity (Fig. S9, ESI†), reducing water and KOH uptake and dimensional swelling (Fig. 2c and Fig. S10, ESI†). M3 exhibited the highest water uptake due to its significantly higher IEC (2.83 mmol g^{-1}) yet maintained acceptable dimensional stability (Fig. 2c). Significantly, the swelling trend in 1 M KOH (Fig. S10, ESI†) is similar to that in pure water but with reduced overall swelling. The increased swelling in pure water results from osmotic water dragging within the membrane.[14] Additionally, the O-PBI component has no alkali-absorbing effect, as pure O-PBI membranes exhibit negligible swelling in 1 M KOH compared to the blend membranes M1, M2, M3, and M4 (Fig. S10, ESI†).

Despite its high IEC, the relatively low swelling of M3 underscores the stabilizing effect of O-PBI in the blend. The dimensional stability of the membranes appears to be primarily influenced by the total O-PBI content, as membranes with the same O-PBI ratio (23 wt%) exhibit comparable swelling behavior despite significant differences in IECs (Fig. 2c and Table S2, ESI†). Despite having the lowest IEC (1.39 mmol g^{-1}), M2 exhibited the highest in-plane swelling (SR_L) and significant water uptake (112 wt%) due to its low O-PBI content (13 wt%). The tensile properties of the membranes revealed that M1, M3, and M4, comprising the same O-PBI amount, exhibit comparable Young's moduli and tensile strengths within the measurement error (Fig. S9, ESI†). In contrast, M2, with the lowest O-PBI content, is the mechanically weakest material (Fig. S9, ESI†).

Notably, the membranes are transparent and homogeneous (Fig. S11, ESI†). Moreover, the microstructure of the blend membranes was investigated utilizing scanning transmission electron microscopy (STEM) after staining the membranes with Na_2WO_4 to enhance mass-thickness contrast (Fig. 2d).[4] All membranes show a comparatively average structure size of 2.7 to 3.0 nm (bright spots, Fig. 2d), corresponding to the nanophase separation between the cationic headgroup and the backbone by the C6-spacer. Only the M2 membranes show bright features on a larger length scale (15.7 nm, marked with labels in Fig. 2d), corresponding to agglomerates of the positive groups of the P2 polymer. The other blend membranes appear homogeneous on a molecular level, indicating no separation between both polymers, which becomes evident when comparing the images at different magnifications (Fig. S6–S8, ESI†).

Next, the blend membranes were used in an AEMWE device to investigate the hydrogen crossover and to compare the membranes to PiperION® as a commercial reference material. Hereby, we focus on the M1, M3, and M4 since M2 exhibited low conductivity, and thus, poor cell performance was expected. Pt/C on a carbon GDL was used as cathodes, and binder-free NiFe-LDH on a Ni mesh (10 μm fiber diameter) as anodes. The polarization curves and high-frequency resistances (HFR) (Fig. 3a) show that M3 had the best cell performance (1.0 A cm^{-2} at 2.0 V) and lowest HFR (0.30 Ω cm^2) across the tested current densities. However, due to varying through-plane swelling (Fig. 2c), the wet thickness in KOH of the membranes differed, complicating the direct comparison to PiperION® (89 μm). Despite this, M3 (64 μm) exhibited significantly lower HFR than M1 (45 μm), aligning with its higher *ex situ* conductivity (Fig. 2b). M4 showed the worst performance (1.0 A cm^{-2} at 2.4 V, 0.50 Ω cm^2), likely due to its lower conductivity and greater thickness (65 μm). Finally, the voltage during the crossover measurement was recorded as an initial indicator of membrane durability in AEMWE (Fig. S16, ESI†).

Different membrane swellings influence mass and charge transport at the membrane-electrode interface, leading to non-overlapping HFR-corrected polarization curves. Moreover, batch variations in NiFe-LDH anodes may affect the results. Interestingly, our previous work using M4 achieved a significantly better *in situ* performance (2.0 A cm^{-2} at 1.8 V).[4] However, this was under different conditions: a smaller active area (5 cm^2), a single-channel serpentine flow field, different catalysts and electrodes, and a different cell compression.[4]

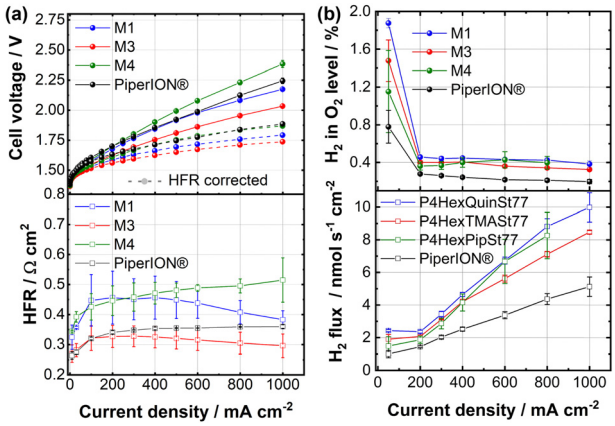

Fig. 3 (a) As-recorded and HFR-compensated polarisation curves (after the hydrogen crossover measurement), and the respective HFRs at each current density. (b) Molar fraction of H_2 in O_2 and the H_2 flux density at each current density. For all tests the membranes used had the following thicknesses: d_{wet}(M1) = 45 μm, d_{wet}(M3) = 64 μm, d_{wet}(M4) = 65 μm, d_{wet}(PiperION®) = 89 μm. All measurements were conducted at 70 °C with 1 M KOH as feed and at ambient pressure.

Open Access Article. Published on 03 December 2024. Downloaded on 8/9/2025 5:24:47 PM.
This article is licensed under a Creative Commons Attribution 3.0 Unported Licence.

This study gives additional attention to assessing hydrogen crossover, a topic rarely reported for AEMs in literature. The hydrogen content in oxygen was measured according to a previously published procedure.[15] For higher current densities, hydrogen dilution due to increased oxygen formation results in lower hydrogen levels, reflecting the expected decrease in H_2 concentration as O_2 production increases.

However, a sharp increase is observed when decreasing the current density from 200 mA cm^{-2} to 50 mA cm^{-2} (Fig. 3b). At higher current densities, a slight decrease in H_2 in O_2 levels is observed for all membranes. At a current density of 0.8 A cm^{-2}, the H_2 in O_2 concentrations are 0.42% for M1, 0.34% for M3, 0.40% for M4, and 0.21% for PiperION. Despite having the highest IEC and water uptake, M3 exhibited superior H_2 crossover properties. This phenomenon may be attributed to three factors: (1) TMA is the least bulky cation, whereas the bulkier Pip and Quin may exhibit higher gas diffusion due to the increased free volume resulting from less dense chain packing.[8] Thus, small cations like TMA may be beneficial in terms of hydrogen barrier properties. (2) In KOH, the swelling is significantly lower than in pure water (65% *vs.* 142%, Fig. S10, ESI†), contributing to the generally low crossover observed for all membranes. (3) The O-PBI content was constant at 23 wt% across all tested membranes. O-PBI is an effective barrier to hydrogen diffusion as a stiff, densely packed polymer with strong interchain interactions.[16,17]

Significantly, the H_2 in O_2 levels rise to roughly 20–45% of the lower explosion limit at 50 mA cm^{-2}, limiting electrolyzers' lower operating point. Compared to recently reported carboxylated SEBS membranes using 15 wt% KOH[18] and polyisatin-derived ion-solvating blend membranes with 20 wt% KOH,[15] these values are within the same order of magnitude. Notably, for all blend membranes reported in this study, substantially lower H_2 in O_2 levels were measured compared to recently reported sulfonated polybenzimidazoles (H_2 in O_2 levels above 1% at current densities between 50 and 300 mA cm^{-2}).[17] Thus, all blend membranes demonstrate excellent hydrogen barrier properties despite their significant water uptake (Fig. 2c), but further improvement toward operation at elevated pressure and increased dynamic range is necessary. Notably, the lower H_2 concentration in O_2 and the reduced H_2 flux for PiperION can be attributed to the substantially thicker PiperION membrane than the blend membranes. The crossover flux (Fig. 3b) shows a linear increase with current density for PiperION, while M3 exhibits a similar linear trend only at current densities above 400 mA cm^{-2}. The other membranes exhibit a non-linear behavior. The increase in H_2 flux across the membrane with rising current density may be attributed to higher hydrogen concentration at the cathode-membrane interface, caused by local supersaturation, as suggested by previous crossover studies in the literature.[15,18]

In conclusion, novel anion-conducting polystyrenes were synthesized by improving the purity of 4-(6-bromohexyl)styrene. Alkaline-stable cationic groups (TMA, Quin, Pip, and Im) were examined for their impact on membrane properties and AEMWE performance. Blending with O-PBI yielded robust membranes, with M3 (77 wt% TMA-functionalized polystyrene, 23 wt% O-PBI) showing the highest hydroxide conductivity (69 mS cm^{-1} at 80 °C and 90% RH) and sufficient dimensional stability. M3 demonstrated low hydrogen crossover and superior performance compared to PiperION®.

Linus Hager: conceptualization, methodology, investigation, data curation, visualization, writing – original draft. Maximilian Schrodt: investigation, writing – review & editing. Manuel Hegelheimer: investigation, writing – review & editing. Julian Stonawski: writing – review & editing. Pradipkumar Leuaa: investigation, writing – review & editing. Christodoulos Chatzichristodoulou: supervision, writing – review & editing. Andreas Hutzler: investigation, writing – review & editing. Thomas Böhm: investigation, writing – review & editing. Simon Thiele: supervision, writing – review & editing. Jochen Kerres: supervision, conceptualization, writing – review & editing, funding acquisition.

The authors thankfully acknowledge the funding from Project SUSTAINCELL. The Clean Hydrogen Partnership and its members, Hydrogen Europe and Hydrogen Europe Research, support the project under Grant Agreement No 101101479.

Data availability

The data supporting this article have been included as part of the ESI.†

Conflicts of interest

There are no conflicts to declare.

Notes and references

1 N. Du, *et al.*, *Chem. Rev.*, 2022, **122**, 11830–11895.
2 N. Chen and Y. M. Lee, *Prog. Polym. Sci.*, 2021, **113**, 101345.
3 F. Dionigi, *et al.*, *ChemSusChem*, 2016, **9**, 962–972.
4 L. Hager, *et al.*, *J. Mater. Chem. A*, 2023, **11**, 22347–22359.
5 X. Z. Lim, *Nature*, 2023, **620**, 24–27.
6 D. Henkensmeier, *et al.*, *J. Electrochem. Energy Convers. Storage*, 2021, 18.
7 H. Khalid, *et al.*, *Membranes*, 2022, **12**, 989.
8 L. Yin, *et al.*, *Angew. Chem., Int. Ed.*, 2024, **63**, e202400764.
9 D. Pan, *et al.*, *ACS Macro Lett.*, 2023, **12**, 20–25.
10 K. Yang, *et al.*, *J. Membr. Sci.*, 2020, **596**, 117720.
11 K. M. Hugar, *et al.*, *J. Am. Chem. Soc.*, 2015, **137**, 8730–8737.
12 J. Fan, *et al.*, *ACS Macro Lett.*, 2017, **6**, 1089–1093.
13 W.-H. Lee, *et al.*, *ACS Macro Lett.*, 2017, **6**, 566–570.
14 O. Boström, *et al.*, *J. Mater. Chem. A*, 2023, **11**, 21170–21182.
15 M. Makrygianni, *et al.*, *J. Membr. Sci.*, 2023, **669**, 121331.
16 J. H. Bitter and A. Asadi Tashvigh, *Ind. Eng. Chem. Res.*, 2022, **61**, 6125–6134.
17 A. Dayan, *et al.*, *Adv. Energy Mater.*, 2023, **13**, 2302966.
18 D. Serhiichuk, *et al.*, *ACS Appl. Energy Mater.*, 2024, **7**, 1080–1091.

 This journal is © The Royal Society of Chemistry 2025